

# Optical energy storage properties of $\text{Sr}_2\text{MgSi}_2\text{O}_7:\text{Eu}^{2+},\text{R}^{3+}$ persistent luminescence materials

Hermi F. Brito · Jukka Hassinen · Jorma Hölsä ·  
Högne Jungner · Taneli Laamanen · Mika Lastusaari ·  
Marja Malkamäki · Janne Niittykoski · Pavel Novák ·  
Lucas C. V. Rodrigues

ESTAC2010 Conference Special Issue  
© Akadémiai Kiadó, Budapest, Hungary 2011

**Abstract** The details of the mechanism of persistent luminescence were probed by investigating the trap level structure of  $\text{Sr}_2\text{MgSi}_2\text{O}_7:\text{Eu}^{2+},\text{R}^{3+}$  materials (R: Y, La-Lu, excluding Pm and Eu) with thermoluminescence (TL) measurements and Density Functional Theory (DFT) calculations. The TL results indicated that the shallowest traps for each  $\text{Sr}_2\text{MgSi}_2\text{O}_7:\text{Eu}^{2+},\text{R}^{3+}$  material above room temperature were always ca. 0.7 eV corresponding to a strong TL maximum at ca. 90 °C. This main trap energy was only

slightly modified by the different co-dopants, which, in contrast, had a significant effect on the depths of the deeper traps. The combined results of the trap level energies obtained from the experimental data and DFT calculations suggest that the main trap responsible for the persistent luminescence of the  $\text{Sr}_2\text{MgSi}_2\text{O}_7:\text{Eu}^{2+},\text{R}^{3+}$  materials is created by charge compensation lattice defects, identified tentatively as oxygen vacancies, induced by the  $\text{R}^{3+}$  co-dopants.

H. F. Brito · J. Hölsä · L. C. V. Rodrigues  
Departamento de Química Fundamental, Universidade de São Paulo, Instituto de Química, Av. Prof. Lineu Prestes, 748, São Paulo, SP CEP 05508-900, Brazil

J. Hassinen · J. Hölsä · T. Laamanen · M. Lastusaari ·  
M. Malkamäki · J. Niittykoski · L. C. V. Rodrigues  
Department of Chemistry, University of Turku, 20014 Turku, Finland

J. Hölsä · M. Lastusaari (✉)  
Turku University Centre for Materials and Surfaces (MatSurf),  
Turku, Finland  
e-mail: miklas@utu.fi

H. Jungner  
Dating Laboratory, University of Helsinki, 00014 Helsinki,  
Finland

T. Laamanen · M. Malkamäki  
Graduate School of Materials Research (GSMR), Turku, Finland

P. Novák  
Institute of Physics, Academy of Sciences of the Czech  
Republic, 16253 Prague 6, Czech Republic

*Present Address:*

J. Niittykoski  
OMG Kokkola Chemicals Oy, P.O. Box 286, 67101 Kokkola,  
Finland

**Keywords** Thermoluminescence · Persistent luminescence · DFT · Disilicate · Trapping

## Introduction

Persistent luminescence materials can emit light several hours after the removal of the irradiation source, usually natural or artificial light or UV radiation. This phenomenon, a special case of thermally stimulated luminescence, results from the storage of energy to traps and its subsequent release induced by the thermal energy available at room temperature [1]. The most efficient persistent luminescence materials, i.e.,  $\text{CaAl}_2\text{O}_4:\text{Eu}^{2+},\text{Nd}^{3+}$  and  $\text{SrAl}_2\text{O}_4:\text{Eu}^{2+},\text{Dy}^{3+}$  [2] as well as  $\text{Sr}_4\text{Al}_{14}\text{O}_{25}:\text{Eu}^{2+},\text{Dy}^{3+}$  [3] and  $\text{Sr}_2\text{MgSi}_2\text{O}_7:\text{Eu}^{2+},\text{Dy}^{3+}$  [4] can continue emitting light in excess of 24 h in the dark. In the daily life, persistent luminescence materials have established an invaluable position with their most obvious application: self-lit signalization. The materials show great potential in other uses as medical diagnostics [5], too.

Numerous papers have been published on the mechanism of persistent luminescence in different  $\text{Eu}^{2+}$  doped materials, but no agreement has been reached, so far [6]. It is well established that the luminescent center in these materials is

the  $\text{Eu}^{2+}$  ion and that the co-doping  $\text{R}^{3+}$  (rare earth) ions affect the efficiency of persistent luminescence, positively or negatively depending on both the host lattice and the dopant. However, the exact modus operandi of the co-doping  $\text{R}^{3+}$  ion as well as that of other lattice defects is uncertain. The  $\text{R}^{3+}$  ions have been suggested to trap holes [7] or electrons [8] or just to create lattice defects [9] due to charge compensation. To be observed, persistent luminescence does not necessarily need the presence of the co-dopants, although there are exceptions as the  $\text{Sr}_3\text{SiO}_5:\text{Eu}^{3+},\text{R}^{3+}$  materials that show persistent luminescence only if selected  $\text{R}^{3+}$  co-dopants are added [10]. Also, it is agreed that the energy storage properties may be simultaneously affected by six different energy schemes: the band gap of the host material ( $E_g$ ), the 4f and 5d ground energy levels of both the  $\text{R}^{2+}$  and  $\text{R}^{3+}$  ions as well as those of different lattice defects as cation and oxygen vacancies. To fully understand the mechanism behind the persistent luminescence needed to enable the design of new more efficient materials, the interplay between these energy level schemes needs to be resolved.

The band gap energy of a material can usually be obtained from luminescence excitation measurements, though only by using synchrotron radiation due to the high energies involved. On the other hand, according to an empirical model [11, 12], the location of the 4f ground levels of divalent rare earths in a particular host lattice can be obtained from luminescence emission spectra by measuring the energy of the charge transfer transition of  $\text{Eu}^{3+}$ , whilst the photoconductivity measurements of  $\text{Ce}^{3+}$  yield the trivalent 4f ground levels. The energy of the 4f–5d transitions of  $\text{Ce}^{3+}$  and  $\text{Eu}^{2+}$  give the locations of the 5d levels. These values have been reported earlier also for the  $\text{Sr}_2\text{MgSi}_2\text{O}_7:\text{Eu}^{2+},\text{R}^{3+}$  materials (Fig. 1) [13, 14]. Finally, the trap energies can be obtained by thermoluminescence (TL) measurements. Unfortunately, TL as such cannot reveal the nature of the traps, i.e., whether they are due to

lattice defects as strontium or oxygen vacancies or to the dopants.

In this work, the optical energy storage properties of the efficient blue emitting  $\text{Sr}_2\text{MgSi}_2\text{O}_7:\text{Eu}^{2+},\text{R}^{3+}$  persistent luminescence materials were studied by a combination of experimental TL data and theoretical DFT (Density Functional Theory) calculations. The aim was to gain more information on which kind species act as the energy reservoirs in these materials.

## Experimental

The polycrystalline  $\text{Sr}_2\text{MgSi}_2\text{O}_7:\text{Eu}^{2+},\text{R}^{3+}$  (R: Y, La-Lu, excluding Pm and Eu) materials were prepared by a solid state reaction between stoichiometric amounts of  $\text{SrCO}_3$  (Merck, Pro Analyti),  $\text{Mg}(\text{NO}_3)_2 \cdot 6\text{H}_2\text{O}$  (Merck, Pro Analyti), fumed  $\text{SiO}_2$  (Sigma, 99.8 %) and rare earth oxides (99.9–99.99 %) using firing for 1 h at 700 °C followed by annealing for 10 h at 1350 °C in a reducing  $\text{N}_2 + 10\% \text{H}_2$  gas sphere. The materials were doped and co-doped with 1 mol-% of the  $\text{Eu}^{2+}$  and  $\text{R}^{3+}$  ions, respectively. The purity of the materials was checked by routine X-ray powder diffraction measurements. Traces of  $\text{Sr}_3\text{MgSi}_2\text{O}_8$  were occasionally observed as impurities.

The TL glow curves were measured with an upgraded Risø TL/OSL-DA-12 system using a constant heating rate of 5 °C s<sup>-1</sup> in the temperature range from 25 to 400 °C. The global TL emission from UV to 650 nm was monitored. Prior to the TL measurements, the samples were irradiated with a combination of the Philips TL 20 W/05 (emission maximum at 360 nm) and TL 20 W/03 (420 nm) UV lamps for 30 s. A delay of 3 min between the irradiation and measurement was used. The analysis of the TL glow curves was carried out by the deconvolution of the TL curves with the program TLanal v.1.0.3 [15] which uses the general approximation (GA) method as a background. The peaks were considered to be of the second-order kinetics because of their symmetric shape.

The electronic structure of the  $\text{Sr}_2\text{MgSi}_2\text{O}_7$  material containing isolated oxygen vacancies was calculated using the WIEN2k package [16]. WIEN2k is based on the full potential linearized augmented plane wave method, an approach which is among the most precise and reliable ways to calculate the electronic structure of solids. The generalized gradient approximation (GGA) was employed. In the calculations, one  $\text{O}^{2-}$  anion per unit cell was replaced by a vacancy. No charge compensation or defect aggregation was considered. The reliable calculation of the electronic structure requires the optimization of the crystal structure including the isolated vacancy. This was achieved by relaxing the atomic positions in the unit cell whilst the lattice parameters were not changed. The crystal structure

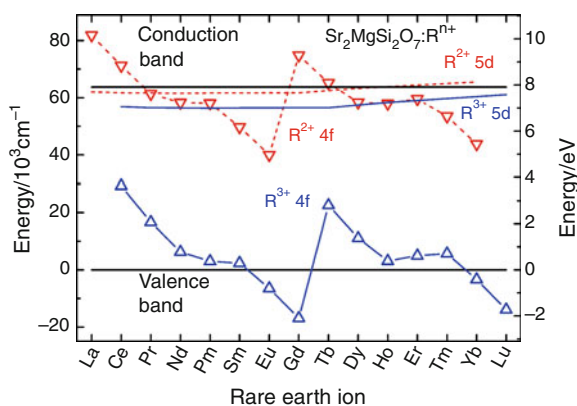


**Fig. 1** Location of the 4f and 5d ground levels of the  $\text{R}^{2+}$  and  $\text{R}^{3+}$  ions in  $\text{Sr}_2\text{MgSi}_2\text{O}_7$  [13] obtained by using the empirical model [11, 12]

of  $\text{Sr}_2\text{MgSi}_2\text{O}_7$  is of the åkermanite ( $\text{Ca}_2\text{MgSi}_2\text{O}_7$ ) type, which belongs to the melilite group of minerals. The structure is tetragonal with the space group  $P4_21m$  (No. 113, Z: 2, a: 7.9957(10), c: 5.1521(9) [17]), and it is composed of layers of corner sharing  $\text{MgO}_4$  and  $\text{SiO}_4$  tetrahedra forming five-membered rings. These layers are held together by eight-coordinated  $\text{Sr}^{2+}$  cations. The structure contains one site for each cation and three oxide sites.

## Results and discussion

### Persistent luminescence and thermoluminescence

All the  $\text{Sr}_2\text{MgSi}_2\text{O}_7:\text{Eu}^{2+},\text{R}^{3+}$  materials, including that without  $\text{R}^{3+}$  co-doping, showed persistent luminescence (Fig. 2). Except for the  $\text{Y}^{3+}$ ,  $\text{Sm}^{3+}$ ,  $\text{Gd}^{3+}$ ,  $\text{Tb}^{3+}$ , and  $\text{Yb}^{3+}$  co-doped materials, all the other co-dopants enhanced the persistent luminescence with respect to the singly doped  $\text{Sr}_2\text{MgSi}_2\text{O}_7:\text{Eu}^{2+}$  material. The extent of enhancement was up to 1.5 orders of magnitude. Also, the relative fading of the persistent luminescence between 1 and 10 min after the removal of the irradiation, i.e., the  $I_{10}/I_1$  ratio, varied significantly, though not as much as the enhancement of the initial intensity. The slowest complete fading of the persistent emission (i.e., the longest duration of persistent luminescence) was observed with  $\text{Dy}^{3+}$  co-doping.

The TL glow curves showed a strong signal at ca. 90 °C for each material (Fig. 3). This signal, being in the temperature range ideal for the persistent luminescence [1], was observed both with and without co-doping and it can thus be considered characteristic to the host lattice. In some materials, e.g., with  $\text{La}^{3+}$  and  $\text{Tm}^{3+}$  co-doping, also significantly deeper traps around 200 °C were observed. This temperature range is typical of those reported for dosimetric materials (e.g., 220 °C for both  $\text{LiF}:\text{Mg,Cu,P}$  [18]

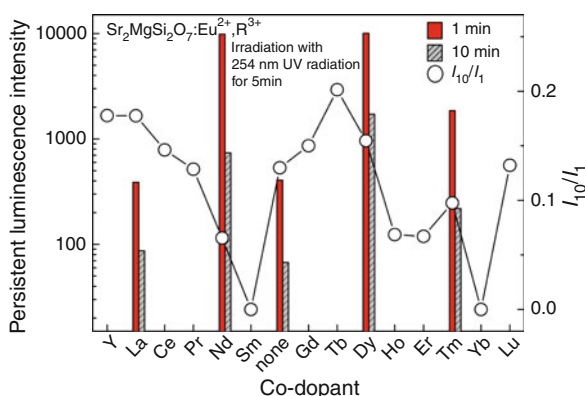


**Fig. 2** Persistent luminescence intensity of the  $\text{Sr}_2\text{MgSi}_2\text{O}_7:\text{Eu}^{2+},\text{R}^{3+}$  materials at 1 and 10 min after the removal of the irradiation source (note the logarithmic intensity scale)

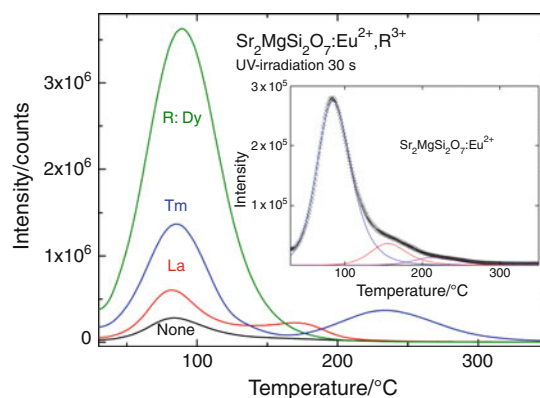


**Fig. 3** Thermoluminescence glow curves of selected  $\text{Sr}_2\text{MgSi}_2\text{O}_7:\text{Eu}^{2+},\text{R}^{3+}$  materials (inset deconvolution of the TL glow curve of  $\text{Sr}_2\text{MgSi}_2\text{O}_7:\text{Eu}^{2+}$ )

and  $\text{CaSO}_4:\text{Dy}^{3+}$  [19] with a heating rate of  $2\text{ °C s}^{-1}$ ) and the corresponding traps can not be emptied to any considerable extent by the thermal energy available at room temperature. The observed TL intensities at 90 °C, on the other hand, correlated well with the persistent luminescence intensity, i.e., the stronger was the TL peak at ca. 90 °C the more intense was the persistent luminescence.

The deconvolution of the TL glow curves indicated that the shallowest traps for each  $\text{Sr}_2\text{MgSi}_2\text{O}_7:\text{Eu}^{2+},\text{R}^{3+}$  material were always ca. 0.7 eV (Fig. 4) corresponding to the strong TL maximum at ca. 90 °C. This main trap energy was only slightly modified by the different co-dopants. On the other hand, the trap densities, i.e., the capacity to store energy to a particular trap, were significantly influenced by the co-dopants (Fig. 4). This suggests

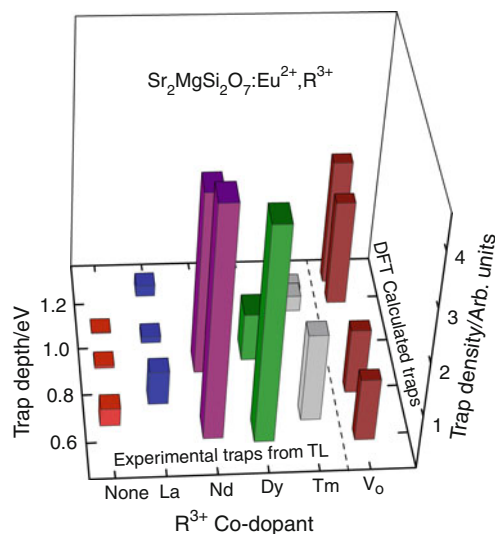


**Fig. 4** Trap depths and densities obtained from TL data for selected  $\text{Sr}_2\text{MgSi}_2\text{O}_7:\text{Eu}^{2+},\text{R}^{3+}$  materials and calculated with DFT by introducing an oxygen vacancy to the non-doped  $\text{Sr}_2\text{MgSi}_2\text{O}_7$  unit cell (Note: the calculated trap densities have not the same scale as the experimental ones)

that either the addition of the co-dopants may create additional traps (enhancing co-dopants) similar to the intrinsic main traps or destroy some of them (quenching co-dopants). It is also possible that the enhancing  $R^{3+}$  co-dopants possess energy levels close to that of the intrinsic trap thus increasing the trap density. The modification of trap energies results from the  $R^{3+}$ -defect interaction. It should be kept in mind that both the co-dopants and the defects created by the charge compensation have relative charges sometimes drastically different from the host cations and anions.

For the best enhancing co-dopants, i.e.,  $Nd^{3+}$ ,  $Dy^{3+}$  and  $Ho^{3+}$ , the  $R^{2+}$  4f ground level is ca. 0.6 eV below the conduction band (Fig. 1), which is very close to the 0.7 eV of the main trap. On the other hand, the fourth best enhancing co-dopant ( $Tm^{3+}$ ) has its  $R^{2+}$  4f ground level at 1.2 eV below the conduction band. This is clearly further away from the main trap energy than those of the three best enhancers. In fact, it is closer to 1.6 eV of the quenching  $Sm^{3+}$ . Considering 1.2 eV in terms of trap depths for second order TL bands, the peak temperature for such a trap would be above 210 °C. This trap would be very difficult to empty at room temperature and no enhancing of persistent luminescence would be expected. It seems that the location of 4f ground level of the  $R^{2+}$  ions may not be of direct significance on the persistent luminescence of the  $Sr_2MgSi_2O_7:Eu^{2+},R^{3+}$  materials.

### Trap identification

It has been reported that for the  $YPO_4:Ce^{3+},R^{3+}$  materials [20], the trend observed for the trap energies by TL measurements is very similar to that for the  $R^{2+}$  4f ground level energies of the respective co-dopants with the difference in absolute energies between the two sets being of the order of 0.5 eV. This suggests that the co-dopant energy levels act as the energy storage traps and that divalent co-dopants are created [21]. These materials present a simple system as there are no defects to be expected due to charge compensation as the trivalent (co-)dopants enter the single  $Y^{3+}$  site in the structure. Instead, the size difference between the  $R^{3+}$  and  $Y^{3+}$  ions can induce important structural distortions and strains.

For the  $Sr_2MgSi_2O_7:Eu^{2+},R^{3+}$  materials, the situation is more complicated. The trivalent co-dopants need charge compensation when entering the  $Sr_2MgSi_2O_7$  lattice as there are no trivalent sites available. Moreover, the reducing conditions used in the preparation of the materials to ensure the reduction of  $Eu^{3+}$  of the  $Eu_2O_3$  starting material to  $Eu^{2+}$  are expected to create oxygen vacancies, i.e., intrinsic defects. The existence of intrinsic defects has been proven by the observation of defect-related luminescence from non-doped  $Sr_2MgSi_2O_7$  at 10 K [22]. Also,

XANES (X-ray Absorption Near Edge Structure) measurements have shown that the co-dopants are always trivalent in the  $Sr_2MgSi_2O_7:Eu^{2+},R^{3+}$  materials [23]. This suggests that if the co-dopants act as electron traps,  $R^{3+}-e^-$  pairs rather than the  $R^{2+}$  species will be created.

Comparing the trap depths obtained from the TL measurements with the energies of the co-dopants'  $R^{2+}$  and  $R^{3+}$  4f ground levels clearly shows that the variation in the trap depths (total spread: ca. 1.5 and spread of the main trap: ca. 0.2 eV along the R series) is far less than that of the ground level energies (ca. 5 eV). However, the evolution of the depths of the main trap at 0.7 eV as a function of the co-dopant does follow a trend similar, albeit less pronounced, to that of the 4f ground levels (Fig. 5). The similarity is closer to the  $R^{3+}$  than the  $R^{2+}$  levels, however. This supports the assumption that the main trap is of intrinsic nature and not due to the co-dopants, and it agrees with the fact that the presence of divalent co-dopants has not been observed.

Other factors which may possibly affect the trap depths to be considered are the size and charge density of the  $R^{3+}$  co-dopants [24]. However, both these factors basically behave in a linear manner in the  $R^{3+}$  series. The present results show that there is a profound disagreement between the evolution of the main trap depth and these linear contributions. Although most of the chemical properties of the rare earths behave linearly across the series, one can find non-linear behaviour in the redox properties of the rare earth ions. The effect of the differences in these properties should be studied, too, but are out of the scope of the present contribution.

The introduction of one isolated oxygen vacancy in the O1, O2 or O3 site in the unit cell of  $Sr_2MgSi_2O_7$  results in the creation of unoccupied levels close to the bottom of the conduction band. These levels may indicate the presence of

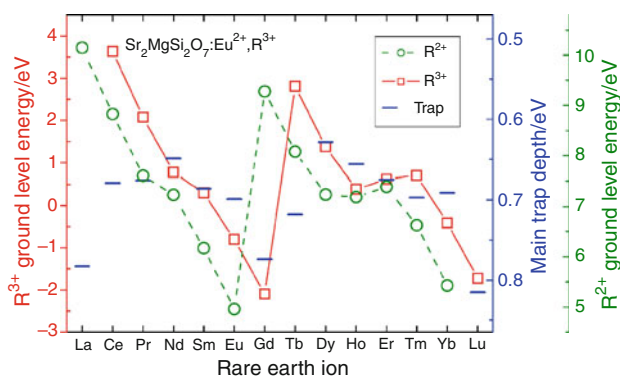


**Fig. 5** Comparison of the trends in main trap (at ca. 0.7 eV) depths of the  $Sr_2MgSi_2O_7:Eu^{2+},R^{3+}$  materials obtained from TL data as well as the  $R^{2+}$  and  $R^{3+}$  4f ground level energies with respect to the top of the valence band [13] obtained using the empirical model [11, 12] (note the different energy scales)

shallow electron trap levels which can be bleached with the thermal energy available at room temperature. The trap levels obtained with the DFT calculations (Fig. 4) range from 5.3 to 6.9 eV above the top of the valence band corresponding to trap depths between 0.2 and 1.8 eV. However, also discrete deep levels close to the valence band (at 1–2 eV above the valence band) were obtained. Nevertheless, prohibitively high amount of energy is required to bleach these deepest traps. The shallowest traps (depths 0.2–0.4 eV) obtained by DFT will be emptied below room temperature and could thus not be observed by the present TL setup. On the other hand, the next group of traps induced by the isolated oxygen vacancies is centered at ca. 0.6 eV below the bottom of the conduction band, which suggest that the main trap present in all the  $\text{Sr}_2\text{MgSi}_2\text{O}_7:\text{Eu}^{2+},\text{R}^{3+}$  materials could be due to an oxygen vacancy. This agrees with the fact that oxygen vacancies should be present even in the non-doped  $\text{Sr}_2\text{MgSi}_2\text{O}_7$  material and that the energy of this trap is only slightly modified by the co-doping.

## Conclusions

Results from the experimental TL measurements and theoretical DFT calculations on the trap levels in  $\text{Sr}_2\text{MgSi}_2\text{O}_7:\text{Eu}^{2+},\text{R}^{3+}$  were successfully combined with the energy level scheme constructed based on the empirical model [11, 12]. New information was obtained on the nature of the trapping sites responsible for the persistent luminescence behavior of the  $\text{Sr}_2\text{MgSi}_2\text{O}_7:\text{Eu}^{2+},\text{R}^{3+}$  materials. The results show that the main trapping site is due to a lattice defect intrinsic to the  $\text{Sr}_2\text{MgSi}_2\text{O}_7$  matrix and that its energy can be only slightly modified by co-doping. Since the trend of the differences in the energy of the shallowest trap is non-linear thus differentiating from most of the properties of the  $\text{R}^{3+}$  ions, the modification may be due to the trap- $\text{R}^{3+}$  4f ground level interaction.

In the future, the DFT calculations will be extended to account also for cation defects,  $\text{R}^{2+}/\text{R}^{3+}$  dopants, and different defect aggregates to study their effect on the trap level structure. The effect of different irradiation energies on the TL glow curves and trap structures will be investigated, too.

**Acknowledgements** Financial support is acknowledged from the Turku University Foundation, Jenny and Antti Wihuri Foundation (Finland) and the Academy of Finland (contracts #117057/2000, #123976/2006, and #134459/2009). The DFT calculations were carried out using the supercomputing resources of the CSC IT Center for Science (Espoo, Finland). The study was supported by the research mobility agreements (112816/2006/JH and 116142/2006/JH, 123976/2007/TL) between the Academy of Finland and the Academy of Sciences of the Czech Republic, as well as the Czech research project AVOZ10100521.

## References

- Aitasalo T, Hölsä J, Jungner H, Lastusaari M, Niittykoski J. Thermoluminescence study of persistent luminescence materials:  $\text{Eu}^{2+}$ - and  $\text{R}^{3+}$ -doped calcium aluminates,  $\text{CaAl}_2\text{O}_4:\text{Eu}^{2+},\text{R}^{3+}$ . *J Phys Chem B*. 2006;110:4589–98.
- Yamamoto H, Matsuzawa T. Mechanism of long phosphorescence of  $\text{SrAl}_2\text{O}_4:\text{Eu}^{2+},\text{Dy}^{3+}$  and  $\text{CaAl}_2\text{O}_4:\text{Eu}^{2+},\text{Nd}^{3+}$ . *J Lumin*. 1997;72–74:287–9.
- Lin Y, Tang Z, Zhang Z, Nan CW. Anomalous luminescence in  $\text{Sr}_4\text{Al}_{14}\text{O}_{25}:\text{Eu},\text{Dy}$  phosphors. *Appl Phys Lett*. 2002;81:996–8.
- Lin Y, Tang Z, Zhang Z, Wang X, Zhang J. Preparation of a new long afterglow blue-emitting  $\text{Sr}_2\text{MgSi}_2\text{O}_7$ -based photoluminescent phosphor. *J Mater Sci Lett*. 2001;20:1505–6.
- de Chermont QL, Chanéac C, Seguin J, Pellé F, Maîtrejean S, Jolivet J-P, Gourier D, Bessodes M, Scherman D. Nanoprobes with near-infrared persistent luminescence for in vivo imaging. *Proc Natl Acad Sci USA*. 2007;104:9266–77.
- Hölsä J. Persistent luminescence beats the afterglow: 400 years of persistent luminescence. *ECS Interface*. 2009;18(4):42–5.
- Matsuzawa T, Aoki Y, Takeuchi N, Murayama Y. A new long phosphorescent phosphor with high brightness,  $\text{SrAl}_2\text{O}_4:\text{Eu}^{2+},\text{Dy}^{3+}$ . *J Electrochem Soc*. 1996;143:2670–3.
- Dorenbos P. Mechanism of persistent luminescence in  $\text{Eu}^{2+}$  and  $\text{Dy}^{3+}$  codoped aluminate and silicate compounds. *J Electrochem Soc*. 2005;152:H107–10.
- Aitasalo T, Dereń P, Hölsä J, Jungner H, Krupa J-C, Lastusaari M, Legendziewicz J, Niittykoski J, Stręk W. Persistent luminescence phenomena in materials doped with rare earth ions. *J Solid State Chem*. 2003;171:114–22.
- Hölsä J, Kotlov A, Laamanen T, Lastusaari M, Malkamäki M, Welter E. Persistent luminescence of  $\text{Sr}_3\text{SiO}_5:\text{Eu}^{2+},\text{R}^{3+}$  (R: Y, La-Nd, Sm, Gd-Lu). In: Proceedings of excited states of transition elements 2010 (ESTE-2010), Piechowice, Poland, September 4–9, 2010. p. 49.
- Dorenbos P. Systematic behaviour in trivalent lanthanide charge transfer energies. *J Phys*. 2003;15:8417–34.
- Dorenbos P. Relation between  $\text{Eu}^{2+}$  and  $\text{Ce}^{3+} f \leftrightarrow d$ -transition energies in inorganic compounds. *J Phys*. 2003;15:4797–807.
- Hölsä J, Niittykoski J, Kirm M, Laamanen T, Lastusaari M, Novák P, Raud J. Synchrotron radiation study of the  $\text{M}_2\text{MgSi}_2\text{O}_7:\text{Eu}^{2+}$  persistent luminescence materials. *ECS Trans*. 2008;6:1–10.
- Dorenbos P. Mechanism of persistent luminescence in  $\text{Sr}_2\text{MgSi}_2\text{O}_7:\text{Eu}^{2+},\text{Dy}^{3+}$ . *Phys Stat Sol B*. 2005;242:R7–9.
- Chung KS. TL glow curve analyzer v. 1.0.3. Korea Atomic Energy Research Institute and Gyeongsang National University, Korea; 2008.
- Blaha P, Schwarz K, Madsen GKH, Kvasnicka D, Luitz J. Schwarz K, editors. WIEN2k, an augmented plane wave + local orbitals program for calculating crystal properties, Vienna University of Technology, Austria, 2001.
- Kimata M. The structural properties of synthetic Sr-åkermanite,  $\text{Sr}_2\text{MgSi}_2\text{O}_7$ . *Z Kristallogr*. 1983;163:295–304.
- Fung KKL. Investigation of dosimetric characteristics of the high sensitivity LiF-Mg, Cu, P thermoluminescent dosimeter and its applications in diagnostic radiology—a review. *Radiography*. 2004;10:145–50.
- Mathur VK, Lewandowski AC, Guardala NA, Price JL. High dose measurements using thermoluminescence of  $\text{CaSO}_4:\text{Dy}$ . *Radiat Meas*. 1999;30:735–8.
- Bos AJJ, Dorenbos P, Bessière A, Viana B. Lanthanide energy levels in  $\text{YPO}_4$ . *Radiat Meas*. 2008;43:222–6.
- Dorenbos P, Bos AJJ, Poolton, NRJ. Electron transfer processes in double lanthanide activated  $\text{YPO}_4$ . *Opt Mater*. 2010 (in press).

22. Aitasalo T, Hassinen J, Hölsä J, Laamanen T, Lastusaari M, Malkamäki M, Niittykoski J, Novák P. Synchrotron radiation investigations of the  $\text{Sr}_2\text{MgSi}_2\text{O}_7:\text{Eu}^{2+}, \text{R}^{3+}$  persistent luminescence materials. *J Rare Earths*. 2009;4:529–38.
23. Carlson S, Hölsä J, Laamanen T, Lastusaari M, Malkamäki M, Niittykoski J, Valtonen R. X-ray absorption study of rare earth ions in  $\text{Sr}_2\text{MgSi}_2\text{O}_7:\text{Eu}^{2+}, \text{R}^{3+}$  persistent luminescence materials. *Opt Mater*. 2009;31:1877–9.
24. Clabau F, Rocquefelte X, Le Mercier T, Deniard P, Jobic S, Whangbo M-H. Formulation of phosphorescence mechanisms in inorganic solids based on a new model of defect conglomeration. *Chem Mater*. 2006;18:3212–20.